



TITLE:

Isolation and characterization of novel high-CO₂-requiring mutants of *Chlamydomonas reinhardtii*.

AUTHOR(S):

Wang, Lianyong; Yamano, Takashi; Kajikawa, Masataka; Hirono, Masafumi; Fukuzawa, Hideya

CITATION:

Wang, Lianyong ...[et al]. Isolation and characterization of novel high-CO₂-requiring mutants of *Chlamydomonas reinhardtii*. Photosynthesis research 2014

ISSUE DATE:

2014-02-19

URL:

<http://hdl.handle.net/2433/182922>

RIGHT:

The final publication is available at link.springer.com; 許諾条件により本文は2015-02-20に公開.; この論文は出版社版ではありません。引用の際には出版社版をご確認ご利用ください。; This is not the published version. Please cite only the published version.

Isolation and characterization of novel high-CO₂ requiring mutants of *Chlamydomonas reinhardtii*

Lianyong Wang¹, Takashi Yamano¹, Masataka Kajikawa¹, Masafumi Hirono², Hideya Fukuzawa¹

¹*Graduate School of Biostudies, Kyoto University, Kyoto, 606-8502, Japan*

²*Graduate School of Science, University of Tokyo, Tokyo, 113-0033, Japan*

Hideya Fukuzawa

Graduate School of Biostudies, Kyoto University, Kyoto, 606-8502, Japan

Phone: +81-75-753-6277

FAX: +81-75-753-9228

E-mail: fukuzawa@lif.kyoto-u.ac.jp

Abstract

Aquatic microalgae induce a carbon-concentrating mechanism (CCM) to maintain photosynthetic activity in low-CO₂ conditions. Although the molecular mechanism of the CCM has been investigated using the single cell green alga *Chlamydomonas reinhardtii*, and several CCM-related genes have been identified by analyzing high-CO₂ (HC)-requiring mutants, many aspects of the CO₂-signal transduction pathways remain to be elucidated. In this study, we report the isolation of novel HC-requiring mutants defective in the induction of CCM by DNA tagging. Growth rates of 20,000 transformants grown under HC and low-CO₂ conditions were compared, and three HC-requiring mutants (H24, H82, and P103) were isolated. The photosynthetic CO₂-exchange activities of these mutants were significantly decreased compared with that of wild-type cells, and accumulation of HLA3 and both LCIA and HLA3 were absent in mutants H24 and H82, respectively. Although the insertion of the marker gene and the HC-requiring phenotype were linked in the tetrad progeny of H82, and a calcium-sensing receptor CAS was disrupted by the insertion, exogenous expression of CAS alone could not complement the HC-requiring phenotype.

Keywords

Chlamydomonas reinhardtii; carbon-concentrating mechanism; CO₂-signal transduction; high-CO₂-requiring mutants

Introduction

Some aquatic photosynthetic organisms possess a carbon-concentrating mechanism (CCM) to maintain optimal photosynthetic activity under CO₂-limiting conditions caused by the slow CO₂ diffusion rate in aquatic environments and the low catalytic capacity of ribulose 1, 5-bisphosphate carboxylase-oxygenase (Rubisco) – the CO₂ fixation enzyme. In *Chlamydomonas reinhardtii*, a single cell green alga, the CCM operates by inducing numerous CCM-related proteins involved in acquiring dissolved inorganic carbon (Ci; CO₂ and HCO₃⁻) from external sources and generating elevated levels of HCO₃⁻ in the stroma (Moroney and Ynalvez 2007). In addition to the environmental Ci concentration, induction of the CCM is also dependent on light intensity (Yamano et al. 2008), although it remains unclear whether a change in light intensity has a direct or indirect effect on the induction process.

In order to concentrate HCO₃⁻ in the chloroplast stroma, a low-CO₂ (LC)-inducible Ci-transport system is needed (Spalding 2008; Wang et al. 2011). Membrane proteins LCI1, LCIA, and HLA3 are considered to associate with Ci transport under LC conditions. LCIA is a member of the Formate/Nitrite Transporter (FNT) family and its transcription level is strongly induced by LC stress (Miura et al. 2004). The expression of LCIA in *Xenopus* oocytes led to uptake activity of NO₂⁻ as well as HCO₃⁻ (Mariscal et al. 2006). LCI1 is localized to the plasma membrane, and exogenous expression of LCI1 under high-CO₂ (HC) conditions showed an increased photosynthetic affinity for Ci and intracellular Ci accumulation (Ohnishi et al. 2010). HLA3 belongs to an ATP-binding cassette (ABC) transporter superfamily and is predicted to localize to the plasma membrane (Im and Grossman 2002). A recent study showed that simultaneous knockdown of *HLA3* and *LCIA* caused a dramatic decrease in

growth rate, photosynthetic C_i affinity, and C_i accumulation, indicating that these proteins are cooperatively associated with C_i transport as part of the CCM (Duanmu et al. 2009).

CCM1 (also known as CIA5) has been identified as a regulatory factor for the induction of *LCII*, *LCIA*, and *HLA3* under LC conditions (Fukuzawa et al. 2001; Xiang et al. 2001; Miura et al. 2004). Moreover, the fact that the induction of almost all LC-inducible genes is impaired in a *ccm1* mutant suggests that CCM1 is a master regulator of the CCM through the LC signal transduction pathway (Miura et al. 2004; Fang et al. 2012). Moreover, downstream of CCM1, the LC-inducible MYB DNA-binding transcriptional regulator LCR1 was identified and shown to function as a transmitter and amplifier of the LC signal from CCM1 to at least three LC-inducible genes, *CAH1*, *LCII*, and *LCI6* (Yoshioka et al. 2004).

Although the function of CCM1 and LCR1 as key regulators of CCM-related genes has been investigated, the full CO_2 -signal transduction pathway remains unclear, possibly because of the small number of regulatory mutants isolated. In this study, we report the isolation of HC-requiring mutants showing retarded growth rates in LC conditions. By examining the photosynthetic characteristics and expression profiles of these CCM-related proteins, the obtained mutants were shown to be defective in C_i transporters.

Materials and methods

Strains and culture conditions

C. reinhardtii strain C9 (photosynthetically wild-type (WT) strain available from the National Institute for Environmental Studies, Japan, as strain NIES-2235) and

CCM1-disrupted mutant C16 (Fukuzawa et al. 1998) were cultured in Tris-acetate-phosphate (TAP) medium for maintenance. For physiological analyses and western blot analyses, cells were first photoautotrophically cultured in a modified high-salt medium (HSM) containing 20 mM MOPS aerated with air enriched with 5% CO₂ (HC conditions) for 12 h. And then, the cultures were diluted five-times with modified HSM and divided into two culture tubes aerated with HC or ordinary air containing 0.04% CO₂ (LC conditions) for 12 h, respectively, at 25°C under continuous illumination at 80 μmol photons m⁻² s⁻¹.

Transformation of cells

A 1,999-bp DNA fragment containing the hygromycin (hyg)-resistant gene *aph7*'' driven by β₂-tubulin promoter was amplified by PCR from plasmid pHyg3 (Berthold et al. 2002) using PrimeSTAR GXL DNA Polymerase (TAKARA BIO, Shiga, Japan) by 35 cycles of denaturation for 10 s at 98°C, annealing for 15 s at 60°C, and extension for 2 min at 68°C with a forward primer (5'-GCACCCCAGGCTTTACACTTTATGCTTCC-3') and reverse primer (5'-CCATTCAGGCTGCGCAACTGTTGG-3'). Similarly, a 1,534-bp DNA fragment containing the paromomycin (par)-resistance gene *aph8*'' driven by *HSP70A* (heat shock protein 70 A)-*RBCS2* tandem promoter (Lodha et al. 2008), was amplified by PCR from plasmid pGenD-aphVIII (Nakazawa et al. 2007) using PrimeSTAR GXL DNA Polymerase by 30 cycles of denaturation for 10 s at 98°C, annealing for 15 s at 60°C, and extension for 2 min at 68°C with a forward primer 5'-GCTTATCGATACCGTCGACCT-3' and reverse primer 5'-AACACCATCAGGTCCCTCAG-3'. The PCR product was purified using a PCR

purification kit (QIAGEN, Valencia, CA, USA) and the concentration was adjusted to $100 \mu\text{g mL}^{-1}$.

Transformation of *C. reinhardtii* cells without cell-wall degradation was performed as reported previously (Yamano et al. 2013). Briefly, C9 cells in early logarithmic phase were collected and transformed by electroporation using a NEPA21 electroporator (NEPAGENE, Chiba, Japan). The transformants were incubated at 25°C for 24 h with gentle agitation under illumination at $1.5 \mu\text{mol photons m}^{-2} \text{s}^{-1}$ and then screened on TAP plates containing $30 \mu\text{g mL}^{-1}$ hyg or $10 \mu\text{g mL}^{-1}$ par at 25°C under $80 \mu\text{mol photons m}^{-2} \text{s}^{-1}$. After 4 days, colonies of transformants appeared and then subjected to the screening process of HC-requiring mutants.

Screening of high- CO_2 -requiring mutants

Cells grown under HC conditions for 12 h were replicated into two 96-well microtiter plates containing liquid HSM medium. One of the plates was incubated in a chamber supplied with LC air and the other in the chamber supplied by HC air for 3 days. Every 24 h, optical density at 700 nm (OD_{700}) was measured using a microtiter plate reader XFluor4 (TECAN, Tokyo, Japan). For the first screening, transformants whose OD_{700} under HC conditions did not reached to 1.0 at 72 h were discarded, and transformants whose OD_{700} under LC conditions was less than five-times of the initial OD_{700} were selected as candidate HC-requiring mutants. For the second screening, the candidate mutants grown in liquid HSM medium under HC conditions were diluted to OD_{430} of 0.15, 0.07, or 0.03, and $3 \mu\text{L}$ of each cell suspension was spotted onto two solid HSM agar plates, and grown in HC or LC chambers for 9 days.

Measurement of light-dependent CO₂-exchange activity and inorganic carbon-dependent photosynthetic oxygen evolution

For measuring light-dependent CO₂-exchange (LCE) activity, harvested cells after growth in HC or LC conditions were suspended in fresh HSM medium at 5 µg Chl mL⁻¹. LCE activity of the cell suspension was measured using an open infrared gas analysis system with 50 ppm CO₂, as described previously (Yamano et al. 2008).

The affinity for Ci was evaluated by measuring the rate of dissolved Ci-dependent photosynthetic oxygen (O₂) evolution. Cells were collected by centrifugation and then resuspended in Ci-depleted 50 mM HEPES-NaOH buffer (pH 7.8) at 15 µg mL⁻¹ chlorophyll. Photosynthetic O₂ was measured using a Clark-type O₂ electrode (Hansatech Instruments, Norfolk, UK) as described previously (Yamano et al. 2008). The maximum O₂-evolving activity, defined as V_{max}, was measured in the presence of 10 mM NaHCO₃.

Immunoblotting analysis

Extracted soluble proteins and membrane proteins suspended in sodium dodecylsulfate (SDS) gel-loading buffer containing 50 mM Tris-HCl (pH 8.0), 25% glycerol (w/v), 2% SDS, and 0.1 M DTT were incubated at 65°C for 10 min or 100°C for 1 min and subsequently centrifuged at 14,000 g for 3 min. The supernatant containing solubilized proteins was subjected to SDS-PAGE analysis. After electrophoresis, proteins were electrophoretically transferred to polyvinylidene difluoride membranes (Bio-Rad, Hercules, CA, USA). Membranes were blocked with 5% (w/v) non-fat skim milk (Wako, Osaka, Japan) in phosphate-buffered saline (PBS). Blocked membranes were washed with PBS containing 0.1% (v/v) Tween-20 (PBS-T) and treated with the

following antibodies in PBS-T: anti-CCM1 antibody (1:5,000 dilution); anti-CAH1 antibody (1:2,500 dilution); anti-CAH3 antibody (1:2,000 dilution); anti-CAH6 antibody (1:2,000 dilution); anti-LCI1 antibody (1:5,000 dilution); anti-HLA3 antibody (1:1,000 dilution); anti-LCIA antibody (1:5,000 dilution); anti-LCIB antibody (1:5,000 dilution); anti-LCIC antibody (1:10,000 dilution); and anti-Histone H3 antibody (1:10,000 dilution). A horseradish peroxidase-conjugated goat anti-rabbit IgG antibody (1:10,000 dilution; GE Healthcare, Milwaukee, WI, USA) was used as a secondary antibody. Immunologically positive signals were visualized using Luminata Crescendo Western HPR substrate (Millipore, Billerica, MA, USA) and detected using an ImageQuant LAS 4000 (Fuji Film, Tokyo, Japan).

Thermal asymmetric interlaced PCR

For the thermal asymmetric interlaced (TAIL) PCR analysis of upstream flanking regions, specific primers UP-3 (5'-GACTCACCTCCCAGAATTCCTGG-3'), UP-2 (5'-TCGTTCCGCAGGCTCGCGTAGG-3'), and UP-1 (5'-TCGAGAAGTAACAGGGATTCTTGTGTCATG-3') were used for primary, secondary, and tertiary reactions, respectively. Similarly, for downstream flanking regions, DP-4 (5'-CTTCGAGGTGTTTCGAGGAGACCC-3'), DP-3 (5'-CGCTGGATCTCTCCGGCTTCACC-3'), and DP-2 (5'-GCCCCCGGCGCCTGATAAGG-3') were used for primary, secondary, and tertiary reactions, respectively. We also used the degenerate primers RMD227 (Dent et al. 2005), A1 (5'-NGTCGASWGANAWGAA-3'), A3 (5'-WGTGNAGWANCANAGA-3'), A4 (5'-TGWGNAGSANCASAGA-3'), and A7 (5'-NTCGASTWTSGWGTT-3') (Liu et al. 1995; Liu and Whittier 1995). The genomic DNA was diluted 10-fold, and 1 μ L aliquots

were used. Primary reactions with 1× GC buffer (TAKARA BIO), 0.2 mM dNTPs, 5 pmol of specific primer, 60 pmol of degenerate primer, and 1 U of LA Taq (TAKARA BIO) were performed under the following conditions: 2 min, 95°C; 5 cycles (1 min, 94°C; 1 min, 62°C; 2.5 min, 68°C); 1 min, 94°C; 3 min, 25°C; ramping over 3 min to 68°C; 2.5 min, 68°C; 15 cycles (30 s, 94°C; 3.5 min, 68°C; 30 s, 94°C; 3.5 min, 68°C; 30 s, 94°C; 1 min, 44°C; 2.5 min, 68°C); 5 min, 68°C. The primary reaction products were diluted 50-fold, and 1 μL aliquots were subjected to secondary reactions with identical components to the primary reaction under the following conditions: 12 cycles (30 s, 94°C; 3.5 min, 68°C; 30 s, 94°C; 3.5 min, 68°C; 30 s, 94°C; 1 min, 44°C; 2.5 min, 68°C); 5 min, 68°C. The secondary reaction products were diluted 50-fold, and 1 μL aliquots were subjected to tertiary reactions with identical components to the primary reaction under identical conditions to the secondary reaction. The tertiary reaction products were separated by agarose gel electrophoresis, fragments were extracted from the gel, and their sequences were analyzed.

For genomic PCR of flanking regions of hyg cassette and sequencing of the upstream and downstream PCR products, primers of F1 (5'-GCGGATCAGATAATACCCCGTA-3'), R1 (5'-AAGAACAGGGGGCTGAGGTAAT-3'), R2 (5'-AGACTGTGAAGCCATGCCCAGGTAGC-3'), UP-S (5'-TCATGTTTGCGGGTTGTGACTG-3'), and DP-S (5'-CCCCGCTCCGTGTAAATGGAGG-3') were used and their locations were depicted in Fig. 4B.

Quantitative real-time PCR

RNA was extracted from cells grown under HC or LC conditions using an RNeasy Plant Mini Kit (QIAGEN) and any remaining genomic DNA was digested with DNase (QIAGEN) in accordance with the manufacturer's instructions. First strand complementary DNA was synthesized using Superscript III Reverse Transcriptase (Life Technology, Carlsbad, CA, USA). Quantitative real-time PCR was performed using SYBR Premix Ex Taq GC (TAKARA BIO) and a LightCycler 480 Instrument (Roche, Mannheim, Germany) in accordance with the manufacturer's instructions. *CBLP* encoding a receptor of activated protein kinase C was used as an internal control. The primers used were *CAS* (5'-CCTCAGCCCCCTGTTCTTCG-3' and 5'-CGCGGATGTCGATCAGCAC-3'), *HLA3* (5'-CGCTCTGCGCAAGTCCTTC-3' and 5'-CGTAGTTGACGTGGGACAGCA-3'), *LCIA* (5'-TCTCCGTGGGAGGCAACATC-3' and 5'-ACAGACCCACGGGGAACACC-3'), *CBLP* (5'-AGGTCTGGAACCTGACCAACT-3' and 5'-AAGCACAGGCAGTGGATGA-3'). The amplification conditions were as follows: 5 min denaturation at 95°C; 40 cycles at 95°C for 10 s, at 55°C for 30 s and at 68°C for 1 min. Melting curves for each PCR product were determined by measuring the decrease in fluorescence with increasing temperature from 60°C to 95°C.

Expression of hemagglutinin epitope-tagged CAS

For constructing the expression plasmid of hemagglutinin (HA) epitope-tagged CAS, genomic region of *CAS* was amplified by PCR with forward primer (5'-CACAACAAGCCCATATGCAGCTTGCTAACGCTCCTCGCCTCGCGGCC-3') and reverse primer (5'-GGTATCGATCGAATTCCGAGCGGGGGCGGGCAGGCGGCGGGTCTGA-3').

The PCR product was cloned into the *Nde*I and *Eco*RI sites of the expression vector pGenD-HA (Nakazawa et al. 2007) using the In-Fusion reaction (Clontech, Mountain View, CA, USA). The resulting fusion protein contained a HA sequence at its C-terminus. HA-tagged CAS was detected by Anti-HA-Peroxidase, High Affinity 3F10 (1:5,000 dilution; Roche).

Tetrad analysis

The tetrad analysis was performed using an inverted microscope (BX41; Olympus, Tokyo, Japan) equipped with a micromanipulator (Narishige, Tokyo, Japan) and a glass needle (Singer Instruments, Somerset, UK) as described previously (Nishimura et al. 2012).

Results

Isolation of high-CO₂-requiring mutants

In screening, HC-requiring mutants were obtained by comparing the growth rates of cells between HC and LC conditions (Fig. 1A). First, to construct insertion mutant libraries, WT strain C9 was transformed with hyg or par resistance cassettes. In total, approximately 20,000 transformants (10,000 for hyg and 10,000 for par resistance) were generated. For the first screening, the OD₇₀₀ of each transformant grown under HC or LC conditions was compared, and 655 transformants showing retarded growth rates under LC conditions were selected as candidate HC-requiring mutants. For the second screening, these candidates were spotted on HSM agar plates and tested for their growth ability under HC or LC conditions, and transformants showing retarded or no growth under LC conditions were selected. As a result, three mutants, designated as H24, H82,

and P103, were isolated as HC-requiring mutants (Fig. 1B). Although the WT cells could grow well under LC conditions as well as HC conditions, the mutants showed little growth under LC conditions.

Photosynthetic characteristics of the mutants

To evaluate the photosynthetic characteristics of the obtained mutants, the light-dependent CO₂-exchange (LCE) activities were measured (Table 1). As a control of HC-requiring mutant, strain C16 deficient in CCM1 was used. Under LC conditions, C16, H24, H82, and P103 showed drastically decreased LCE activities of 19.7 (16.3%), 10.9 (9.1%), 13.5 (11.2%), and 19.7 (16.4%) $\mu\text{mol CO}_2 \text{ mgChl}^{-1} \text{ h}^{-1}$, respectively, compared with 120.2 $\mu\text{mol CO}_2 \text{ mgChl}^{-1} \text{ h}^{-1}$ for WT cells (Table 1), suggesting lower Ci uptake activity under LC conditions.

Next, the rates of photosynthetic O₂ evolution under changing external Ci concentrations were measured (Fig. 2 and Table 1). Under LC conditions, C16, H82, and P103 showed much higher photosynthetic K_{0.5} (Ci) values of 482.0, 525.6, and 312.4 μM , respectively, compared with a WT value of 48.8 μM , indicating that photosynthetic affinity for Ci was drastically decreased in the mutants. In contrast, LC-acclimated H24 showed typical photosynthetic responses of cells expressing the CCM in the range of 10 to 100 μM Ci and showed approximately 70% of maximal photosynthetic rate at 100 μM Ci. Although the photosynthetic rate of WT cells reached a maximum at 100 μM Ci and retained its activity, the photosynthetic rate of H24 did not increase and attenuated between 100 and 500 μM Ci. The rates then increased again at higher concentrations of Ci, reaching a maximum at 1.5 mM Ci. Although this biphasic response of the photosynthetic curve caused an apparent decrease in the K_{0.5}

(Ci) value of 50.4 μM , attenuated photosynthetic activity between 100 μM and 500 μM , which corresponds to LC conditions, could cause the retarded growth of H24.

Accumulation of carbon concentrating mechanism-related proteins

It was speculated that the absence of some CCM-related proteins led to the HC-requiring phenotype of the mutants. To examine the accumulation of CCM-related proteins, soluble or membrane proteins were extracted from WT, C16, H24, H82, and P103 cells grown under HC or LC conditions. These protein samples were probed with antibodies against CCM-related proteins, including CCM1, CAH1, CAH3, CAH6, LC11, HLA3, LCIA, LCIB, and LCIC (Fig. 3).

In the P103 mutant, CCM1 was not detected, and the accumulation profiles of CCM-related proteins were quite similar to that of C16, suggesting that P103 could be a *CCM1* mutant. By sequencing the genomic region of *CCM1* in P103, a deletion of adenine in the second exon was found (AAAAA in WT and AAAA in P103), causing a frame shift, producing truncated CCM1 with 161 amino acid residues.

In the WT cells, CCM1, CAH3, and CAH6 were accumulated constitutively irrespective of the environmental CO_2 conditions. Although CCM1 and CAH6 accumulated normally in H24 and H82 cells, a slight decrease in CAH3 was observed in C16, H24, H82, and P103 cells. Accumulation profiles of LCIB and LCIC in H24 and H82 cells were similar to that of WT cells with slight accumulation under HC conditions and induced accumulation under LC conditions, as reported previously. HLA3 and LCIA are LC-inducible membrane proteins associated with Ci transport. In LC-acclimated H24 and H82 cells, accumulation of HLA3 or both HLA3 and LCIA, respectively, were not detected.

Genetic linkage between the high-CO₂-requiring phenotype and insertion site of a hygromycin resistance cassette in H82 mutant cells

In order to evaluate a genetic link between the HC-requiring phenotype and insertion of the hyg resistance cassette, H82 cells were crossed with WT strain CC-1690 or CC-125. In total, 96 progenies generated from 24 complete tetrads (A-L from H82×CC-1690 in Supplementary Fig. S1 and M-X from H82×CC-125 in Supplementary Fig. S2) were obtained, and the linkage between the HC-requiring phenotype and hyg resistance was analyzed (Fig. 4A). All progenies showing the HC-requiring phenotype possessed a hyg insertion detected by PCR, suggesting that the mutation in H82 appeared to be caused by a single insertion event.

To determine the flanking region of the hyg cassette, TAIL-PCR was performed. Using UP and DP primers located in the promoter region and 3'-untranslated region (UTR) of the hyg cassette, respectively, both sides of the insertion were sequenced. Comparison of the obtained nucleotide sequence with the *C. reinhardtii* genomic sequence database Phytozome v.9.1 yielded a match to locus *Cre12.g497300* encoding CAS, a calcium-sensing receptor (Fig. 4B). Specifically, the obtained sequence from the UP side matched with a sequence in the 4th intron and that from the DP side matched with a sequence in the 5th exon, correlating with a deletion of 92-bp in CAS. The F1/R1 primer set, homologous to the 4th intron and 5th exon, amplified PCR products of 365-bp from WT and of approximately 7-kb from H82, confirming the hyg insertion in CAS. Considering that the length of the hyg cassette was 1,999-bp, three or four copies of the cassette could be tandemly inserted. Hyg insertion was also confirmed by PCR using several primer sets of F1/UP-S (Fig 4C), DP-S/R1

(Supplementary Fig. S1), and DP-S/R2 (Supplementary Fig. S2).

To investigate whether exogenous expression of *CAS* could complement the HC-requiring phenotype of H82, two independent lines expressing HA-tagged *CAS* (#10 and #13) were isolated (Fig. 4D). In these strains, however, LC-inducible accumulation of *LCIA* and *HLA3* were not complemented. Quantitative real-time PCR also confirmed that LC-inducible expression of *LCIA* and *HLA3* was not complemented in spite of a significant level of accumulation of exogenous HA-tagged *CAS* protein.

Discussion

Rapid construction of insertion mutant libraries using a square pulse electroporator

This study showed the isolation of novel HC-requiring mutants defective in induction of the CCM. Although several studies have reported the screening of *C. reinhardtii* mutants by DNA tagging (Prieto et al. 1996; Fukuzawa et al. 1998; Dent et al. 2005), making insertion mutant libraries has been a time-consuming process. In this study, we firstly used a square electric pulse-generating electroporator for constructing of the libraries. Because of its high efficiency of transformation and speed from preparing cells without removing the cell wall (Yamano et al. 2013), constructing libraries could become a non-limiting step for mutants screening studies.

Relationship between the absence of inorganic carbon transporters and high-CO₂-requiring phenotype

The slow growth rates and decreased LCE activity of the obtained mutants under LC conditions indicated that supplying HC is essential for survival (Fig. 1B). Among the CCM-related proteins examined, only *HLA3* was missing in H24. It was reported that

knockdown of *HLA3* alone resulted in only modest decreases in photosynthetic Ci affinity and Ci uptake at neutral pH conditions (Duanmu et al. 2009). In spite of this result, H24 cells could not grow under LC condition, as shown in spot tests performed at pH 7.0. This was possibly because the completely absence of HLA3 accumulation in H24 mutant caused a more severe phenotype than achieved with knockdown of *HLA3*. Alternatively, we cannot rule out the possibility that the absence of HLA3 was not the main cause of the HC-requiring phenotype, and the accumulation of other proteins related with CCM or photorespiration could be missed. In the H82 mutant, LCIA as well as HLA3 was not accumulated under LC conditions (Fig. 3). Considering that simultaneous knockdown of *HLA3* and *LCIA* resulted in dramatic decreases in growth, Ci uptake, and photosynthetic Ci affinity (Duanmu et al. 2009), the HC-requiring phenotype of H82 could be mainly caused by the absence of LCIA and HLA3. *LCIA*, *HLA3*, and *CAS* are located on chromosome 6, 2, and 12, respectively, and the HC-requiring phenotype of H82 mutant was closely linked with the hyg cassette insertion into *CAS* gene on chromosome 12 (Supplementary Fig. S1 and S2). From those results, it is probable that *LCIA* and *HLA3* themselves were not structurally disrupted in the H82 mutant, although experimental validation is required. Because the transcription of *LCIA* and *HLA3* was also suppressed in H82 (Fig. 4E), the genes responsible for H82 could be a transmitter of the LC signal from CCM1 to at least *LCIA* and *HLA3*, which would be analogous to the function of LCR1 for the regulation of LCI1 (Yoshioka et al. 2004).

To identify the gene responsible for the phenotype of H82, its tetrad progenies were characterized, and it was shown that the *CAS* gene was disrupted by the insertion of hyg cassette. In a previous knockdown analysis of the *CAS* gene, *CAS* was shown to be involved in the acclimation to the high-light (HL) stress particularly by regulating

LHCSR3 expression (Petroutsos et al. 2011) and the Ca^{2+} -dependent regulation of cyclic photosynthetic electron flow of photosynthesis (Terashima et al. 2012). Considering the fact that cyclic photosynthetic electron flow activity was increased under LC conditions (Lucker and Kramer 2013), the expression of *LHCSR3* was regulated by LC as well as HL (Yamano et al. 2008), and the HL has a effect on induction of the CCM as LC conditions (Yamano et al. 2008), it is reasonable to say that CAS could be associated with the cross-talk between HL and LC stress. Unfortunately, HA-tagged CAS introduced into H82 could not complement the HC-requiring phenotype as well as the expression of *HLA3* and *LCIA* under LC conditions (Fig. 4E). Based on these results, it is possible that the HC-requiring phenotype and suppression of *LCIA* and *HLA3* under LC conditions was not attributed to the disruption of CAS alone. However, we could not exclude the possibilities that exogenously expressed HA-tagged CAS could not function *in vivo* because of the addition of HA-tag to the C-terminal end of CAS and that the disruption of other gene along with CAS could be attributed to the phenotype of H82. As far as tetrad progenies tested were concerned, *hyg* insertion into CAS determined by PCR was closely linked with the HC-requiring phenotype of H82 (Supplementary Fig. S1 and S2), suggesting that the genetic locus responsible for the HC-requiring phenotype could be located near to CAS. Considering the case of point mutation of *CCM1* in the P103 mutant, we cannot rule out the possibilities that there could be point mutations, large-scale deletions, rearrangements, or insertion of small portion of *hyg* cassette which could not detected by TAIL-PCR or Southern blot analysis in the responsible gene of H82 mutant.

For identifying the responsible genes of mutants, complementation assay using genomic libraries constructed from bacterial artificial chromosome clones is

useful approach (von Gromoff et al. 2008). Additionally, massive data generated by whole genome sequencing succeeded in the determination of point mutation sites of the *Chlamydomonas* flagella mutants (Lin et al. 2013). Further analyses including these techniques would reveal the disrupted gene responsible for the HC-requiring phenotype of H82 mutant and whether the actual mutation causes the absence of LCIA and HLA3 or not.

Acknowledgements

We thank Dr. Yoshiki Nishimura for technical help and assistance with the tetrad analysis. We also thank Dr. Haru-aki Yanagisawa for providing the expression vectors, pGenD-aphVIII and pGenD-HA. We also thank Dr. Tan Inoue and Dr. Yoshihiko Fujita for letting us use the quantitative real-time PCR system, LightCycler 480. This work was supported by the Promotion of Science (JSPS) KAKENHI (Grant Nos 23120514, 22380059, and 25120714 to H.F., and 25840109 to T.Y.) and the Japan Science and Technology Agency (JST), Advanced Low Carbon Technology Research and Development Program (ALCA).

References

- Berthold P, Schmitt R, Mages W (2002) An engineered *Streptomyces hygrosopicus aph* 7" gene mediates dominant resistance against hygromycin B in *Chlamydomonas reinhardtii*. *Protist* 153:401–412
- Dent RM, Haglund CM, Chin BL, Kobayashi MC, Niyogi KK (2005) Functional genomics of eukaryotic photosynthesis using insertional mutagenesis of *Chlamydomonas reinhardtii*. *Plant Physiol* 137:545–556
- Duanmu D, Miller AR, Horken KM, Weeks DP, Spalding MH (2009) Knockdown of limiting-CO₂-induced gene *HLA3* decreases HCO₃⁻ transport and photosynthetic C_i affinity in *Chlamydomonas reinhardtii*. *Proc Natl Acad Sci USA* 106:5990–5995
- von Gromoff ED, Alawady A, Meinecke L, Grimm B, Beck CF (2008) Heme, a plastid-derived regulator of nuclear gene expression in *Chlamydomonas*. *Plant Cell* 20:552–567
- Fang W, Si Y, Douglass S, Casero D, Merchant SS, Pellegrini M, Ladunga I, Liu P, Spalding MH (2012) Transcriptome-wide changes in *Chlamydomonas reinhardtii* gene expression regulated by carbon dioxide and the CO₂-concentrating mechanism regulator CIA5/CCM1. *Plant Cell* 24:1876–1893
- Fukuzawa H, Ishizaki K, Miura K, Matsueda S, Matsueda S, Ino-ue T, Kucho K, Ohyama K (1998) Isolation and characterization of high-CO₂ requiring mutants from *Chlamydomonas reinhardtii* by gene tagging. *Can J Bot* 76:1092–1097
- Fukuzawa H, Miura K, Ishizaki K, Kucho KI, Saito T, Kohinata T, Ohyama K (2001) *Ccm1*, a regulatory gene controlling the induction of a carbon-concentrating mechanism in *Chlamydomonas reinhardtii* by sensing CO₂ availability. *Proc Natl Acad Sci USA* 98:5347–5352

- Im CS, Grossman AR (2002) Identification and regulation of high light-induced genes in *Chlamydomonas reinhardtii*. *Plant J* 30:301–313
- Lin H, Nauman NP, Albee AJ, Hsu S, Dutcher SK (2013) New mutations in flagellar motors identified by whole genome sequencing in *Chlamydomonas*. *Cilia* 2:14
- Liu YG, Mitsukawa N, Oosumi T, Whittier RF (1995) Efficient isolation and mapping of *Arabidopsis thaliana* T-DNA insert junctions by thermal asymmetric interlaced PCR. *Plant J* 8:457–463
- Liu YG, Whittier RF (1995) Thermal asymmetric interlaced PCR: Automatable amplification and sequencing of insert end fragments from P1 and YAC clones for chromosome walking. *Genomics* 25:674–681
- Lodha M, Schulz-Raffelt M, Schroda M (2008) A new assay for promoter analysis in *Chlamydomonas* reveals roles for heat shock elements and the TATA box in *HSP70A* promoter-mediated activation of transgene expression. *Eukaryot Cell* 7:172–176
- Lucker B, Kramer DM (2013) Regulation of cyclic electron flow in *Chlamydomonas reinhardtii* under fluctuating carbon availability. *Photosynth Res* 117:449–459
- Mariscal V, Moulin P, Orsel M, Miller AJ, Fernández E, Galván A (2006) Differential regulation of the *Chlamydomonas* *Nar1* gene family by carbon and nitrogen. *Protist* 157:421–433
- Miura K, Yamano T, Yoshioka S, Kohinata T, Inoue Y, Taniguchi F, Asamizu E, Nakamura Y, Tabata S, Yamato KT, Ohyama K, Fukuzawa H (2004) Expression profiling-based identification of CO₂-responsive genes regulated by CCM1 controlling a carbon-concentrating mechanism in *Chlamydomonas*. *Plant Physiol* 135:1595–1607
- Moroney JV, Ynalvez R (2007) Proposed carbon dioxide concentrating mechanism in

- Chlamydomonas reinhardtii*. Eukaryot Cell 6:1251–1259
- Nakazawa Y, Hiraki M, Kamiya R, Hirono M (2007) SAS-6 is a cartwheel protein that establishes the 9-fold symmetry of the centriole. Curr Biol 17:2169–2174
- Nishimura Y, Shikanai T, Nakamura S, Kawai-Yamada M, Uchimiya H (2012) Gsp1 triggers the sexual developmental program including inheritance of chloroplast DNA and mitochondrial DNA in *Chlamydomonas reinhardtii*. Plant Cell 24:2401–2414
- Ohnishi N, Mukherjee B, Tsujikawa T, Yanase M, Nakano H, Moroney JV, Fukuzawa H (2010) Expression of a low CO₂-inducible protein, LCI1, increases inorganic carbon uptake in the green alga *Chlamydomonas reinhardtii*. Plant Cell 22:3105–3117
- Petroutsos D, Busch A, Janssen I, Trompelt K, Bergner SV, Weinl S, Holtkamp M, Karst U, Kudla J, Hippler M (2011) The chloroplast calcium sensor CAS is required for photoacclimation in *Chlamydomonas reinhardtii*. Plant Cell 23:2950–2963
- Prieto R, Pardo JM, Niu X, Bressan RA, Hasegawa PM (1996) Salt-sensitive mutants of *Chlamydomonas reinhardtii* isolated after insertional tagging. Plant Physiol 112:99–104
- Spalding M (2008) Microalgal carbon-dioxide-concentrating mechanisms: *Chlamydomonas* inorganic carbon transporters. J Exp Bot 59:1463–1473
- Terashima M, Petroutsos D, Hüdig M, Tolstygina I, Trompelt K, Gäbelein P, Fufezan C, Kudla J, Weinl S, Finazzi G, Hippler M (2012) Calcium-dependent regulation of cyclic photosynthetic electron transfer by a CAS, ANR1, and PGRL1 complex. Proc Natl Acad Sci USA 109:17717–17722
- Wang Y, Duanmu D, Spalding MH (2011) Carbon dioxide concentrating mechanism in *Chlamydomonas reinhardtii*: inorganic carbon transport and CO₂ recapture. Photosynth Res 109:115–122

- Xiang Y, Zhang J, Weeks DP (2001) The *Cia5* gene controls formation of the carbon concentrating mechanism in *Chlamydomonas reinhardtii*. *Proc Natl Acad Sci USA* 98:5341–5346
- Yamano T, Miura K, Fukuzawa H (2008) Expression analysis of genes associated with the induction of the carbon-concentrating mechanism in *Chlamydomonas reinhardtii*. *Plant Physiol* 147:340–354
- Yamano T, Iguchi H, Fukuzawa H (2013) Rapid transformation of *Chlamydomonas reinhardtii* without cell-wall removal. *J Biosci Bioeng* 115:691–694
- Yoshioka S, Taniguchi F, Miura K, Inoue T, Yamano T, Fukuzawa H (2004) The novel Myb transcription factor LCR1 regulates the CO₂-responsive gene *Cah1*, encoding a periplasmic carbonic anhydrase in *Chlamydomonas reinhardtii*. *Plant Cell* 16:1466–1477

Figure legends

Fig. 1 Screening of high-CO₂ (HC)-requiring mutants. (A) Schematic illustration of screening process. PCR-amplified hygromycin (hyg) or paromomycin (par) resistance cassettes were introduced into wild-type (WT) cells by electroporation. Colonies of transformants were picked up, cultured in 96-well microtiter plates under HC conditions, and replicated into two plates. One replicate plate each was incubated under HC or low-CO₂ (LC) conditions, and candidate HC-requiring mutants were screened by measuring optical density (1st screening). Reproducibility of the HC-requiring phenotype was checked by a spot test experiment (2nd screening). (B) Spot test of WT and HC-requiring mutants H24, H82, and P103. Cells grown to logarithmic phase were diluted to the indicated optical density (OD₄₃₀ 0.15, 0.07, or 0.03), 3 μ L of the cell suspensions were spotted on HSM plates and incubated for 9 days in growth chambers supplied with HC or LC under continuous light at 120 μ mol photons m⁻² s⁻¹. H24 and H82 were hyg resistant and P103 was par resistant.

Fig. 2 Oxygen-evolving activity of wild-type (WT) and transformants in response to external dissolved Ci concentrations. WT and mutants were grown in high-CO₂ (HC; closed circles) or low-CO₂ (LC; open circles) conditions. Photosynthetic oxygen evolution was measured using a Clark-type oxygen electrode in the presence of various concentrations of NaHCO₃. Insets show plots at external dissolved Ci concentrations below 500 μ M.

Fig. 3 Accumulation of CCM-related proteins. Accumulation of CCM-related proteins in wild-type (WT), C16, H24, H82, and P103 cells was analyzed by protein

immunoblotting analysis. Cells were first grown under high-CO₂ (HC) condition for 12 h and shifted to HC or low-CO₂ (LC) conditions for 12 h. Histone H3 was used as a loading control. Asterisks indicate the non-specific protein bands.

Fig. 4 Molecular characterization of the H82 mutant. (A) Genetic linkage of the hygromycin (hyg) insertion and high-CO₂ (HC)-requiring phenotype. Genomic DNA was extracted from tetrad progeny (A1-A4) from crosses of H82 and CC-1690. Genomic PCR was performed with the primer sets depicted in (B). For spot test, progenies grown to logarithmic phase were diluted to the indicated optical density (OD₄₃₀ 0.15, 0.07, or 0.03), 3 μ L of each suspension was spotted onto HSM plates, and incubated in a growth chamber supplied with low-CO₂ (LC). Genetic linkage of each tetrad progeny is shown in Online Resource 1. (B) Schematic representation of the hyg cassette insertion into the genome of the H82 mutant. The untranslated region, exon and hyg cassette are shown as white, black, and gray boxes, respectively. Binding sites of PCR primers are indicated by arrows (not drawn to scale). (C) Confirmation of hyg insertion by genomic PCR. Genomic DNA was extracted from wild-type (WT) and H82 cells, and genomic PCR was performed using the primer sets depicted in (B). M indicates the DNA size marker. (D) Accumulation of HA-tagged CAS (CAS-HA), LCIA, and HLA3 in the WT, H82, and CAS-HA-expressing strains #10 and #13. Asterisk indicates a non-specific protein band. (E) Quantitative real-time PCR of *CAS*, *LCIA*, and *HLA3* in WT, H82, and CAS-HA-expressing strains #10 and #13. The expression levels of *CAS*, *LCIA*, and *HLA3* are shown as white, black, and gray bars, respectively.

Supplementary Fig S1. Genetic linkage analysis of the hygromycin (hyg) insertion and high-CO₂ (HC)-requiring phenotype. Genomic DNA was extracted from tetrad progeny (A-L) from crosses of H82 and CC-1690. Genomic PCR was performed with the primer sets (F1 and UP-S or R1 and DP-S) depicted in Fig. 4B. For spot test, progenies grown to logarithmic phase were diluted to the indicated optical density (OD₄₃₀ 0.15, 0.07, or 0.03), 3 μ L of each suspension was spotted onto HSM plates, and incubated in a growth chamber supplied with LC for 4 days.

Supplementary Fig S2. Genetic linkage analysis of the hygromycin (hyg) insertion and high-CO₂ (HC)-requiring phenotype. Genomic DNA was extracted from tetrad progeny (M-X) from crosses of H82 and CC-125. Genomic PCR was performed with the primer set (DP-S and R2) depicted in Fig. 4B. For spot test, progenies grown to logarithmic phase were diluted to the OD₄₃₀ of 0.07, 3 μ L of each suspension was spotted onto HSM plates, and incubated in a growth chamber supplied with HC or LC for 6 days. For hyg resistance test, progenies were directly streaked onto TAP plates containing 30 μ g mL⁻¹ hyg, and incubated under HC condition for 6 days.

Table 1 Photosynthetic parameters of wild-type (WT) and mutants cells

Strain	CO ₂	CO ₂ -exchange activity	V _{max} of O ₂ -evolving	K _{0.5} (Ci) [μM]
name	conditions	[μmol CO ₂ mgChl ⁻¹ h ⁻¹]	activity	
			[μmol O ₂ mgChl ⁻¹ h ⁻¹]	
WT	HC	28.8 ± 10.8	184.7 ± 13.2	298.7 ± 43.3
	LC	120.2 ± 6.1	197.7 ± 18.7	47.8 ± 5.8
C16	HC	26.4 ± 2.5	195.3 ± 19.0	675.9 ± 75.9
	LC	19.7 ± 4.4	245.5 ± 24.0	482.0 ± 27.8
H24	HC	22.2 ± 5.5	102.6 ± 2.0	149.6 ± 69.2
	LC	10.9 ± 5.2	92.0 ± 8.5	50.4 ± 9.1
H82	HC	27.6 ± 1.4	184.6 ± 27.4	425.2 ± 17.5
	LC	13.5 ± 5.2	179.5 ± 12.3	525.6 ± 75.1
P103	HC	13.7 ± 0.9	N.D.	N.D.
	LC	19.7 ± 2.0	168.8 ± 11.1	312.4 ± 9.9

Data are shown ± standard deviation, which were obtained from at least three independent experiments. Ci, inorganic carbon; HC, high CO₂; LC, low CO₂; N.D.; not determined; V_{max}, maximum O₂-evolving activity.

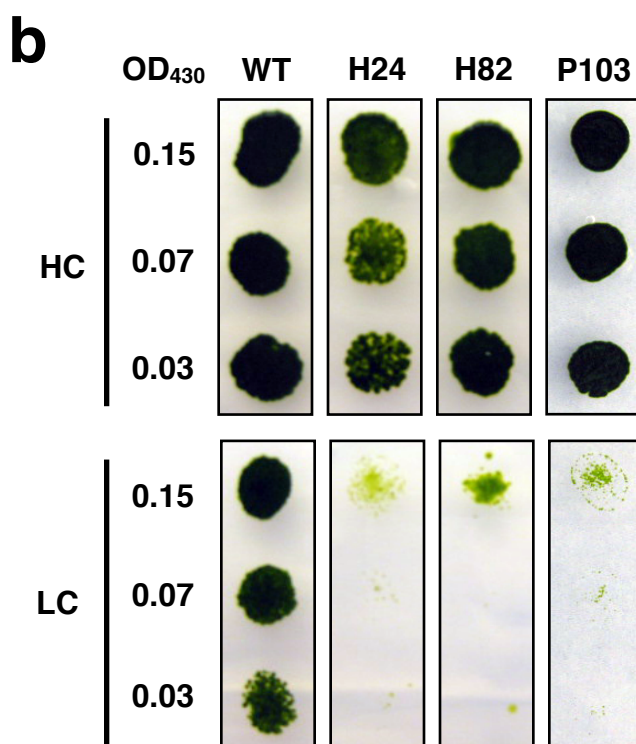
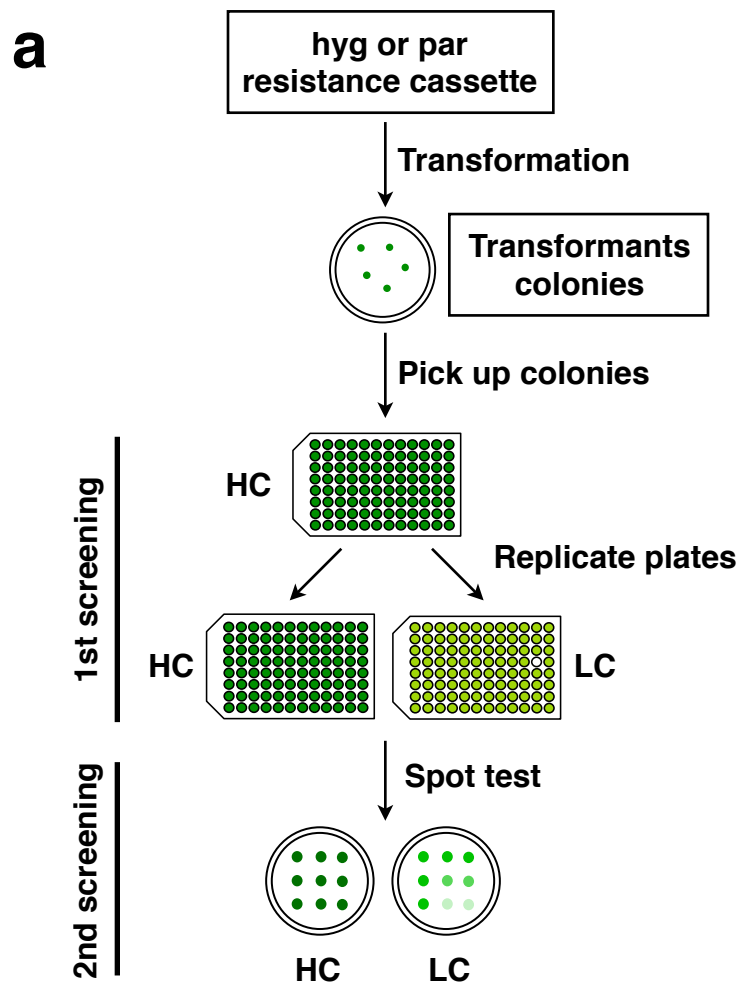


Figure 1

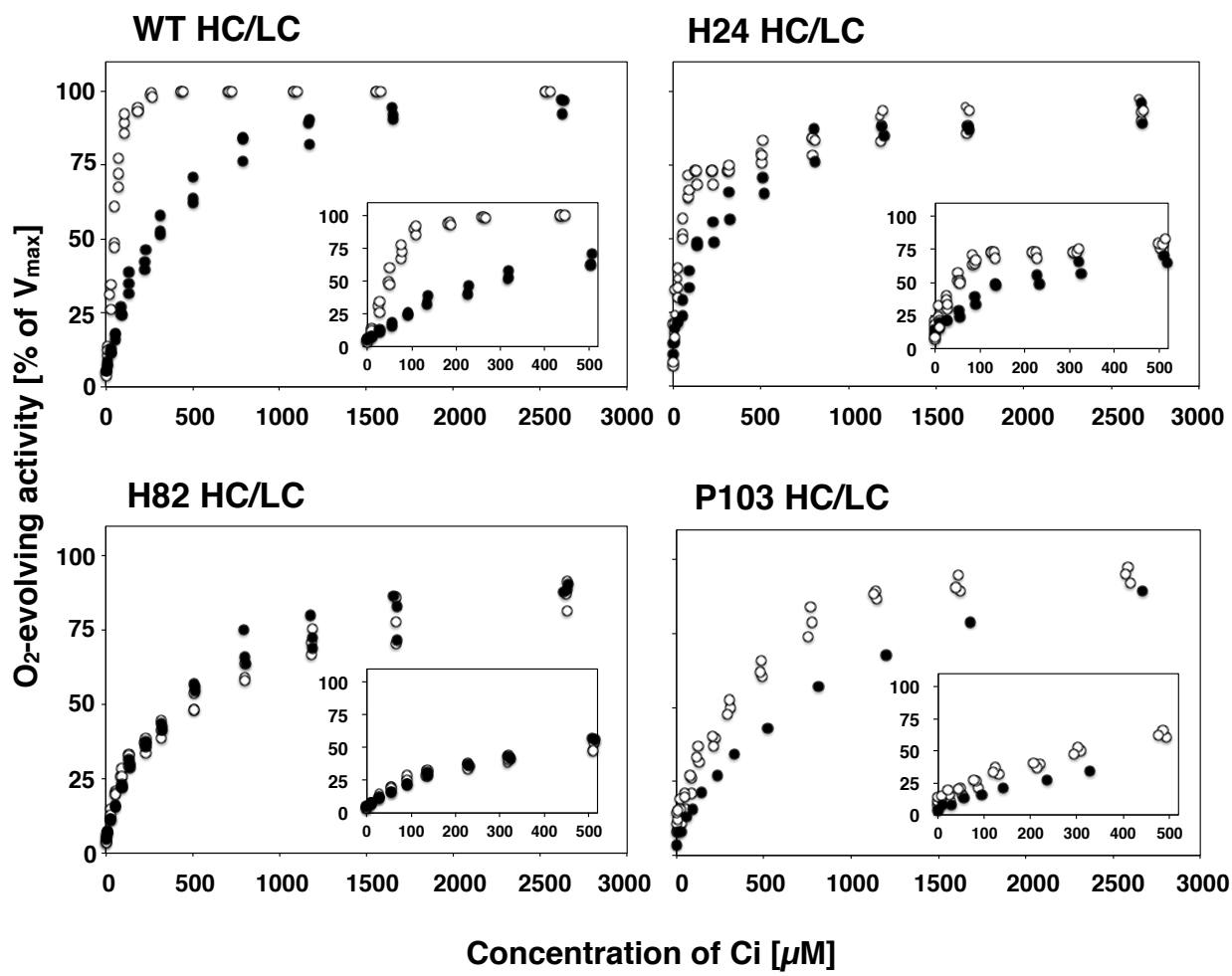


Figure 2

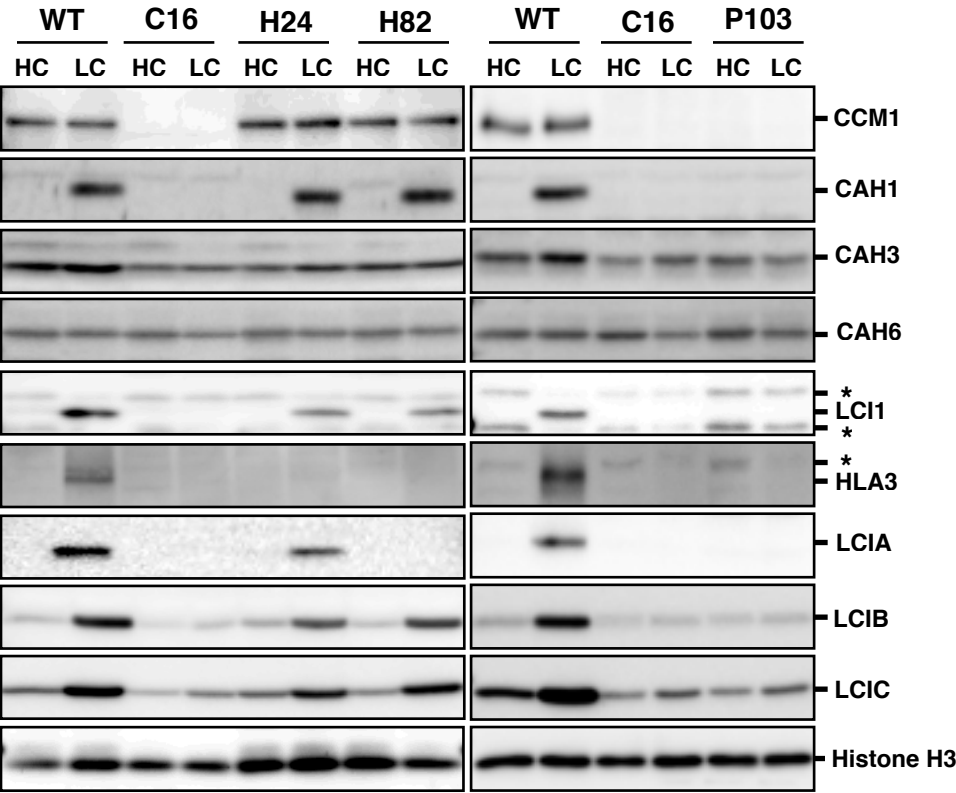


Figure 3

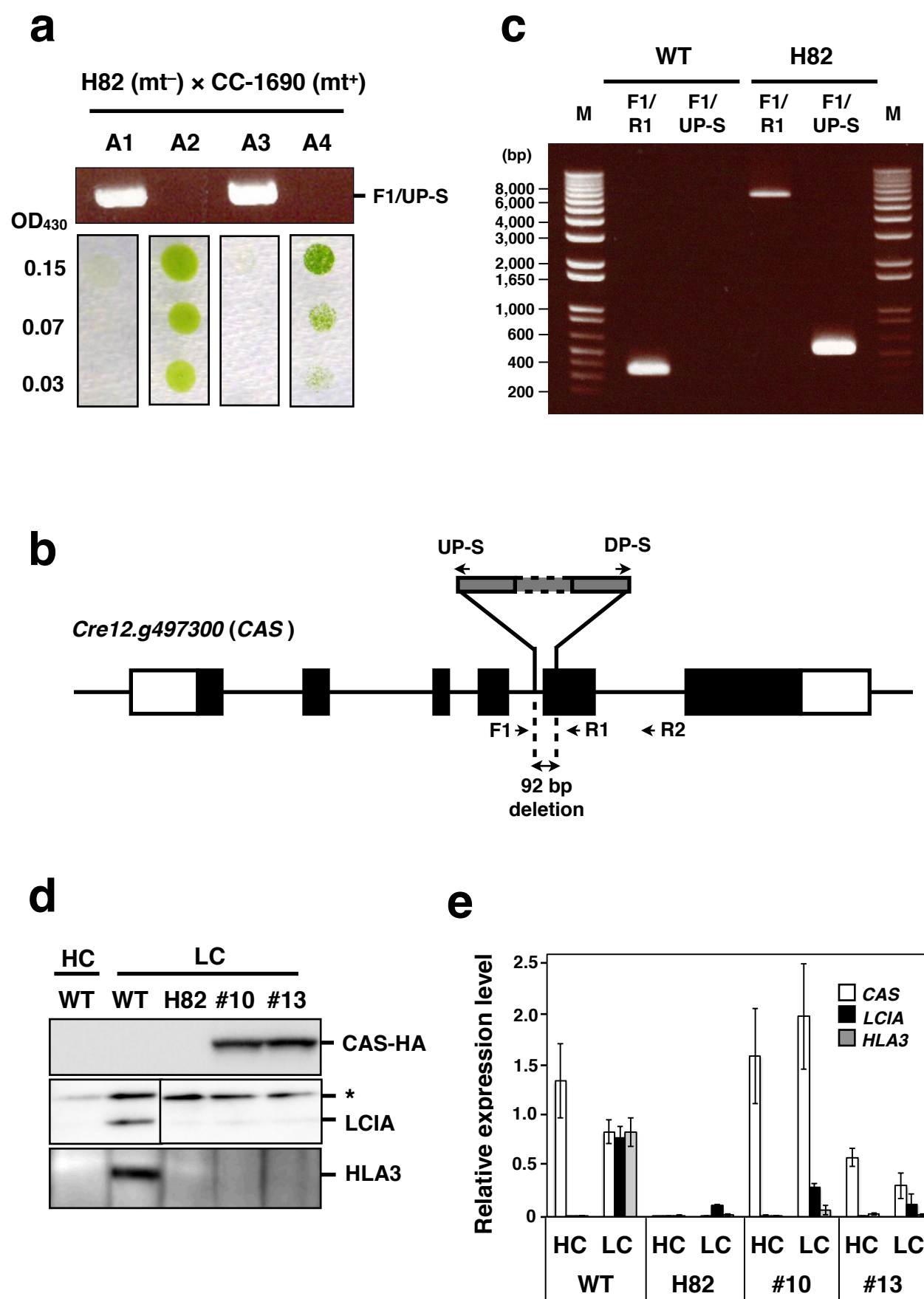


Figure 4

